Progress in Oceanography 147 (2016) 1–9

Contents lists available at ScienceDirect

Progress in Oceanography

journal homepage: www.elsevier.com/locate/pocean

Spatial distributions of polyunsaturated aldehydes and their biogeochemical implications in the Pearl River Estuary and the adjacent northern South China Sea

Zhengchao Wu, Qian P. Li *

State Key Laboratory of Tropical Oceanography, South China Sea Institute of Oceanology, Chinese Academy of Sciences, Guangzhou, China

ARTICLE INFO

Article history:
Received 10 January 2016
Received in revised form 16 July 2016
Accepted 18 July 2016
Available online 25 July 2016

ABSTRACT

This study reports the first comprehensive exploration of the spatial patterns of dissolved and particulate polyunsaturated aldehydes (PUAs), their physical and biological controlling factors, and their potential biogeochemical influences in the Pearl River Estuary (PRE) of the northern South China Sea (NSCS). High levels of total particulate PUAs (0–41 nM) and dissolved PUAs (0.10–0.37 nM) were observed with substantial spatial variation during an intense summer phytoplankton bloom outside the PRE mouth. We found the particulate PUAs strongly correlated with temperature within the high chlorophyll bloom, while showing a generally positive correlation with chlorophyll-*a* for the entire region. Additionally, the Si/N ratio significantly correlated with the particulate PUAs along the estuary suggesting the important role of silica on PUA production in this region. The dissolved PUAs counterparts exhibited a positive correlation with chlorophyll-*a* within the high chlorophyll bloom, but a negatively one with temperature outside, reflecting the essential bio-physical coupling effects on the dissolved PUAs distributions in the ocean. Biogeochemical implications of PUAs on the coastal ecosystem include not only the deleterious restriction of high PUAs-producing diatom bloom on copepod population, but also the profound influence of particulate PUAs on the microbial cycling of organic carbon in the NSCS.

1. Introduction

In recent decades, polyunsaturated aldehydes (PUAs) have attracted increasing attention as these metabolites may play an important role in chemically mediated planktonic interactions and thus regulators of phytoplankton bloom dynamics in the ocean (Miralto et al., 1999; Frost, 2005). The presence of PUAs in seawater, mostly derived from oxidation of fatty acids of phytoplankton cells, may affect a number of processes over various trophic levels, including bacteria production (Edwards et al., 2015), phytoplankton growth (Ribalet et al., 2007a), zooplankton grazing (Jüttner, 2005), as well as fertilization, embryonic development, and larval survival of marine invertebrates (Tosti et al., 2003; Caldwell, 2009). Marine diatoms are believed to be the major phytoplankton producing PUAs in response to their physiological stresses, including growth limitation, competition, and predation (Ianora and Miralto, 2010). Diatom PUA production, however, would depend not only on the organism's physiological state, but also on the species and strains of diatoms, with only 36% of the major diatom species capable of producing PUAs (Wichard et al., 2005a).

While results from culture and laboratory experiments have been criticized for using PUA concentrations orders of magnitude higher than their natural levels in the seawater (Ribalet et al., 2007a; Wichard et al., 2008), there are still few attempts to address the influence of PUAs on various levels of food webs in natural marine ecosystems (Balestra et al., 2011). Until recently, there are very few field PUA measurements available to understand the actual variations of PUAs under in situ conditions (Vidoudez et al., 2011a; Bartual et al., 2014; Morillo-Garcia et al., 2014; Ribalet et al., 2014). It is now recognized that nanomolar and sub-nanomolar concentrations of PUAs are released as particulate and dissolved fractions in the ocean after diatom cell disruption due to zooplankton feeding or cell lysis during phytoplankton blooms (Vidoudez et al., 2011a; Ribalet et al., 2014). The dissolved PUAs (*d*PUA) in seawater would be important for shaping community structure and function of the planktonic ecosystem (Ribalet et al., 2014), whereas the particulate PUAs (*p*PUA) could affect the ocean carbon cycle by stimulating the remineralization of sinking organic matter, decreasing the efficiency of carbon export, and shoaling the depth of nutrient regeneration (Edwards et al., 2015).

The Pearl River Estuary (PRE), one of the largest estuaries in the northern South China Sea (NSCS), is strongly influenced by coastal outflows and seawater intrusion (Mao et al., 2004). As the river

* Corresponding author.
E-mail address: qianli@scsio.ac.cn (Q.P. Li).

http://dx.doi.org/10.1016/j.pocean.2016.07.010
0079-6611/

plume develops, the limiting nutrient for phytoplankton growth shifts from phosphorus in the estuarine waters to nitrogen in the oceanic waters (Zhang et al., 1999; Yin et al., 2001). An intense phytoplankton bloom near the estuary mouth outside the PRE has become a perennial phenomenon due to increasing inorganic carbon and nutrient inputs (Cai et al., 2004; Yin et al., 2004a) associated with the coastal current along the east of Guangdong, and the mixing between the Pearl River outflows and the offshore seawater. The phytoplankton community here is largely dominated by diatoms such as *Skeletonema costatum* (Huang et al., 2004; Harrison et al., 2008). Copepods, the major mesozooplankton of the PRE, are relatively abundant (Tan et al., 2004) and copepod grazing is an important factor for regulating phytoplankton production and size structure of the coastal NSCS (Liu et al., 2010).

In this paper, we present the first comprehensive survey of PUAs during an intense phytoplankton bloom in the PRE of the NSCS. The field study was carried out from the inner estuary to the open sea during the wet season of June 2015 when there was strong mixing between the high nutrient freshwater and the offshore oligotrophic seawater. Along with water-column physical and biogeochemical measurements, we quantified both the dissolved and the particulate PUAs in the surface waters. Our goal was to examine the spatial patterns of particulate and dissolved PUAs in the PRE and their controlling factors while transecting from the eutrophic estuarine waters to the low productivity shelf sea. By comparing the PUA distributions with those of physical, biological, and biogeochemical observations, we explore the relationship between seawater PUAs and bulk water properties and investigate the influence of PUA variability on planktonic ecosystem and biogeochemistry of the PRE and the adjacent NSCS.

2. Materials and methods

2.1. Descriptions of field campaigns and sampling approaches

The Pearl River has three major branches: the west river, the north river, and the east river at the top of the estuary, and a number of small rivers in the river delta area. The largest water discharge of the PRE passes through Modaomen, west of Macau and Humen near the upper estuary, with a total annual sediment delivery of ~80 Mt (Harrison et al., 2008). Two field surveys aboard two private research ships were conducted in the PRE and the adjacent NSCS, the first cruise (QXQ) during June 11th–15th, 2015 and the second cruise (ZJK) during June 17th–26th, 2015 (Fig. 1). Discrete water samples, at 2–4 depths at each station depending on the bottom depth, were collected in 5 L Niskin bottles attached to a nylon hydrocable. Pressure, temperature and conductivity were measured by YSI sensors. For chlorophyll-*a* sampling, 500 mL of water sample were gently filtered (<50 mmHg) through a GF/F (Whatman, GE Healthcare, UK) filter, which was subsequently wrapped in aluminum foil and stored at −20 °C on board. Nutrient samples for nitrate plus nitrite, phosphate, and silicate were frozen immediately after a 0.8 μm Nucleopore filtration. These frozen nutrient samples were stored at −20 °C until final analyses by a Seal AA3 nutrient autoanalyzer (Bran-Luebbe, GmbH) after the cruises. Particulate and dissolved PUAs were sampled in surface waters at 43 stations in the PRE, as chlorophyll maxima were generally found in the surface layer.

2.2. Determination of chlorophyll-a and dissolved nutrients

Chlorophyll-*a* samples were sonicated for 20 min and extracted in 5 mL 90% acetone at 4 °C in the dark for 24 h. These samples were centrifuged at 4000 rpm for 10 min before final determinations by standard fluorescence methods (Parsons et al., 1984) using a Turner Designs fluorometer. Concentrations of nitrate plus nitrite ($NO_3 + NO_2$), phosphate (PO_4), and silicate (SiO_4) were determined by colorimetric methods (Hansen and Koroleff, 1999). Since our study region covers both freshwater and seawater, it was important to correct the nutrient data for salt effects. The influence of salt on nutrient measurements was quantified by using the oligotrophic surface seawater of the central NSCS as nutrient-free seawater (NFSW). A salinity series was made by diluting NFSW with deionized water (DIW). We made a regression between the absorbance of these nutrient free samples after color development (converted to concentration based on standard curves) and their salinity (S) to generate a salt effect correction equation. Salt effect of nitrate can be estimated by $NO_3 = 0.001 \times S + 0.039$, $r^2 = 0.798$. For phosphate, $PO_4 = 0.018 \times S$, $r^2 = 0.989$. For silicate, $SiO_4 = 0.00046 \times S + 0.00359$, $r^2 = 0.994$. All nutrient data were corrected for salt effects based on the sample's salinity and the derived salt effect equation.

2.3. Sample collections, pretreatments, and measurements of particulate PUA

We used a modified protocol of *p*PUA collection and pretreatments (Wichard et al., 2005b; Vidoudez et al., 2011a; Ribalet

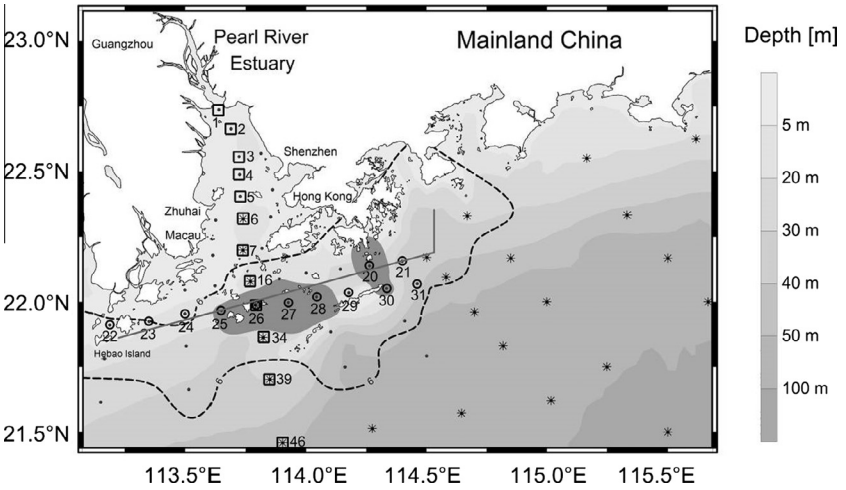

Fig. 1. Sampling map of the Pearl River Estuary and the northern South China Sea. Gray scales are bathymetry; dash curve represents the isoline for surface chlorophyll-*a* of 6 μg L^{-1}, with dark patches highlighting the high chlorophyll region (>10 μg L^{-1}); dots are ZJK stations during June 17th–26th, 2015 with stars for QXQ stations during June 11th–15th, 2015; squares and circles are stations in the along-PRE section in Fig. 3 and across-PRE section in Fig. 4, respectively; the gray line shows the position of a section conducted in July 1999 by Huang et al. (2004).

et al., 2014). Seawater (1 L) was filtered through a GF/C filter (Whatman, GE Healthcare, UK) under vacuum (500 mbar). The filter was then rinsed with 1 mL of a 25 mM *O*-(2,3,4,5,6-pentafluorobenzyl) hydroxylamine hydrochloride (PFBHA·HCl) (Aladdin, China) solution in 0.1 M Tris-HCl buffer (pH of 7.2). The suspended cells were collected in a 4 mL glass vial. After addition of 5 μL of an internal standard (benzaldehyde 10 mM in methanol, Aladdin), the vial was tightly capped and shaken for 5 min. The samples were frozen (in liquid nitrogen) and thawed three times, successively, in order to mechanically break the phytoplankton cells. After on board derivation reaction for 2 h, the *p*PUA samples were frozen in liquid nitrogen and stored at −20 °C until further analysis.

In the lab, the frozen sample was thawed in 1 mL methanol before mixing with 2 mL hexane. The sample was then transferred to a 5 mL EP freezing tube and vortexed for 1 min. Six drops of concentrated sulfuric acid (>95%) were added to the sample by a glass Pasteur pipette, and the sample was vortexed again for 1 min. After centrifugation (Eppendorf centrifuge, Germany) for 10 min at 4000 rpm at room temperature, the hexane phase was collected and transferred into another 2.5 mL EP tube (drying over anhydrous sodium sulphate). With the solvent removed under vacuum, the sample was dissolved in 300 μL hexane and transferred to another 0.5 mL EP tube. The hexane extract was dried again and redissolved in 80 μL hexane before being transferred to a 200 μL glass insert in a 2 mL glass vial. The final concentration was determined by an Agilent 7890A gas chromatography coupled with an Agilent 5975C mass spectrometer (Agilent Technologies Inc., USA). A standard series (0, 0.1, 0.2, 0.5, 1.0, 5.0, 10, 20 nmol/L) was prepared for three major PUAs, including heptadienal (>90%, Aladdin), octadienal (95%, Sigma-Aldrich), and decadienal (85%, Aladdin), by adding certain amounts of these chemicals (in 1 mM methanolic solution) to 1 mL of a 25 mM PFBHA·HCl solution in 0.1 M Tris-HCl (pH 7.2). After injection of 5 μL internal standard (10 mM benzaldehyde in methanol), the mixture was incubated for 1 h at room temperature before being processed through all the sample pretreatment steps. The unit for *p*PUA is nM (nmol PUA from cells in 1 L).

2.4. Sample collections, pretreatments and measurements of dissolved PUA

For *d*PUAs, filtrate (~1 L) collected from the GF/C filtration described in Section 2.3 was passed through a 0.22 μm Nucleopore filter to remove all particulates. A volume of 5 μL of an internal standard (benzaldehyde, 10 mM in methanol) was then added to the filtrate sample. The sample was transferred to a 3 mL C18 solid phase extraction cartridge (Agela Technologies, China), pretreated with 1 mL of a 25 mM PFBHA·HCl solution in 0.1 M Tris-HCl buffer (pH of 7.2), via a Teflon tube with a flow rate of ~1 L h^{-1}. The cartridge was further eluted into a glass vial filled with 3 mL of a 10 mM PFBHA·HCl solution in methanol. After incubation for 2 h at room temperature, these samples were stored at −20 °C until further analysis.

Derivatives of *d*PUAs were extracted and measured by similar methods for *p*PUAs (Section 2.3). Previous studies applied the same calibration curves for both particulate and dissolved PUA derivatives (Vidoudez et al., 2011a). However, the derivation protocol of PUA standards made for the particulate PUA derivatives may be inappropriate for their dissolved counterparts as they have gone through substantially different experimental processes. In order to improve accuracy, we constructed calibration curves for dissolved PUA derivatives separately. A standard series of 0, 0.01, 0.05, 0.1, 0.5, 1.0 nM of heptadienal, octadienal, and decadienal were prepared before each analysis by diluting a certain amount of the PUA stock solution (methanolic solution) with DIW. These standard solutions were subjected to the same experimental procedures as the dissolved PUA derivation method mentioned above, including C18 cartridge absorption, elution, extraction, and GC/MS analysis. The calibration curve for the dissolved PUA derivatives was based on linear regression of the integrated peak areas and the standard PUA concentrations. The unit for *d*PUA is nmol/L of sample solution.

2.5. Estimation of PUA-producing diatom carbon biomass

Diatoms and copepods generally dominate the plankton community of the PRE during summer (Harrison et al., 2008; Liu et al., 2010). Unfortunately, we did not have concurrent measurements of diatom and copepod abundances during our cruises. However, the summer diatom bloom is a perennial phenomenon in the PRE mouth, with a relatively constant phytoplankton composition based on field measurements from 2000 to 2012 (Wei et al., 2012; Zhang et al., 2014; Li et al., 2014). We therefore chose to reanalyze a previously published data conducted in July 1999 (Yin et al., 2001), which conducted a similar cross-estuary section outside the PRE mouth. *Skeletonema costatum*, *Nitzschia pungens*, *Nitzschia delicatissima*, and *Leptocylindrus danicus* are four most abundant diatom groups in the PRE with *S. costatum* generally representing over 50% of the phytoplankton cell counts (Huang et al., 2004; Zhang et al., 2014). Biomasses (μgC L^{-1}) of the four major diatoms were calculated by multiplying the cell carbon (μgC $cell^{-1}$) of each diatom group by its cell abundance (cells L^{-1}). The average cell carbon values for the four diatoms are 22.5 pgC $cell^{-1}$, 86.9 pgC $cell^{-1}$, 21.1 pgC $cell^{-1}$, and 123 pgC $cell^{-1}$, respectively (Harrison et al., 2015). Data from *S. costatum*, *N. delicatissima*, and *L. danicus* were combined as the carbon biomass of PUA-producing diatoms (Miralto et al., 1999; Dutz et al., 2008).

Data of copepod abundance during the summers of 1999, 2006, 2010 and 2011 (Tan et al., 2004; Zhang et al., 2014, 2013) near the PRE mouth were included to explore the general relationship between copepod abundance and PUA-producing diatom biomass within the summer chlorophyll bloom. In order to compare copepod abundance from various cruises, data of Tan et al. (2004) were scaled down by 11 fold to account for the difference of mesh sizes between large (505 μm) and medium (160 μm) zooplankton nets (Lian et al., 2013).

2.6. Statistical analysis

Data analysis was performed using the statistical software SPSS (SPSS version 13.0, SPSS Inc., Chicago, IL) with figures constructed using Microsoft Excel 2003. The Pearson correlation analysis was applied to the concentrations of PUAs and environmental variables, and probabilities (p) of <0.05 were considered to be significant. Comparisons between environmental conditions and PUA concentrations were conducted using reduced major axis model II regression. A solid line in the figures shows a model II linear regression of the plotted data with r representing the Pearson coefficient of correlation. We assumed both regression variables to be independent of each other. A permutation test was carried out to determine the significance of the slopes and to calculate the Pearson coefficients of correlation.

3. Results and discussion

3.1. Spatial distributions of hydrography, chlorophyll-a, and nutrients

Our study region was largely influenced by river discharge as indicated by the surface salinity distribution. An intense river plume developed just outside the PRE mouth (Fig. 2A), likely a

result of complex interactions among buoyancy discharge, tidal forcing, and wind-driven circulation (Zu et al., 2014). The path of the river plume in our surveys resembled that previously identified by Pan et al. (2014) in June 2012, with freshwater flowing from the inner estuary to the west side of the estuary mouth in the south of Macau and then spreading eastward to the NSCS (Fig. 2A). Riverine impacts on the PRE hydrography can be found in the along-estuary section with a gradual increase in temperature from ~26 °C to ~32 °C and salinity from 0 to ~35 (Fig. 3A). Although generally higher salinity water was outside the PRE mouth, there were lower salinity waters found at stations 20 and 30 (Fig. 4A) due to a small filament of riverine outflow through the Hong Kong channel from the east of the PRE mouth (Fig. 2A).

In contrast to low chlorophyll concentrations offshore (<0.5 μg/L), substantially higher chlorophyll-*a* concentrations were observed in the PRE (2–6 μg/L), with the highest values (>10 μg/L) located near the coast. Two chlorophyll patches (>10 μg/L) could be clearly identified, with one outside the PRE mouth including stations 25, 26, 27 and 28, and the other in the south of Hong Kong, including stations 20 and 30 (Fig. 1), indicating an intense phytoplankton bloom. The two patches were separated by relatively higher salinity but lower nutrient waters on the east side of the PRE (Fig. 2B and C), likely from the intrusion of offshore seawaters. Surface nutrient distributions were similar to that of salinity, with decreasing nitrate and silicate along the path of the river plume from the estuary to the sea (Fig. 2B and C). Consistent with previous reports (Zhang et al., 1999; Cai et al., 2004), the Pearl River outflow was highly eutrophic with nitrate >150 μM, silicic acid >120 μM, and phosphate >1.5 μM. High molar ratios in N/P of >100 and Si/P of >80 in the inner estuary (Fig. 3D) supported the potential phosphorus limitation of phytoplankton growth within the estuary (Zhang et al., 1999; Yin et al., 2001).

Although the Si/N ratio of the surface water showed an increasing trend from the inner estuary to the offshore, both N/P and Si/P ratios generally decreased (Fig. 3D). The N/P ratios of the surface waters gradually decreased from >80 in the inner estuary, to ~40 in the middle estuary, to ~20 just outside the estuary mouth, and to <10 in the offshore NSCS (Fig. 3D). The N/P ratios of the cross-estuary section outside the PRE mouth (Fig. 4D) were on average 24 ± 9 (n = 12), which is close to the Redfield ratio of 16 indicating relief of community phosphorus stress. Extremely low Si/P and Si/N ratios were found for station 29 with a very low chlorophyll concentration, likely reflecting silica limitation of diatom growth (Brzezinski, 2008).

3.2. Spatial distributions of particulate PUAs in the surface waters

Our results suggest that particulate octadienal (*p*C8) was the most important component of the total particulate PUAs (T-*p*PUA) in the PRE (on average 71.9%, Fig. 2F and H) with particulate heptadienal (*p*C7) and decadienal (*p*C10) accounting for relatively small fractions (11.2% and 16.9%, Fig. 2E, G, and H). High C8-to-C7 ratios have been reported in P-limited cultures of the diatom *Skeletonema marinoi* (Ribalet et al., 2009), which is the major source of C7 and C8 during coastal blooms (Vidoudez et al., 2011a). Therefore, it is not surprising that we found high *p*C8 but low *p*C7 in the PRE, given the dominance of *S. costatum* (also referred as *S. marinoi*, Sarno et al., 2005) in a P-limited estuary

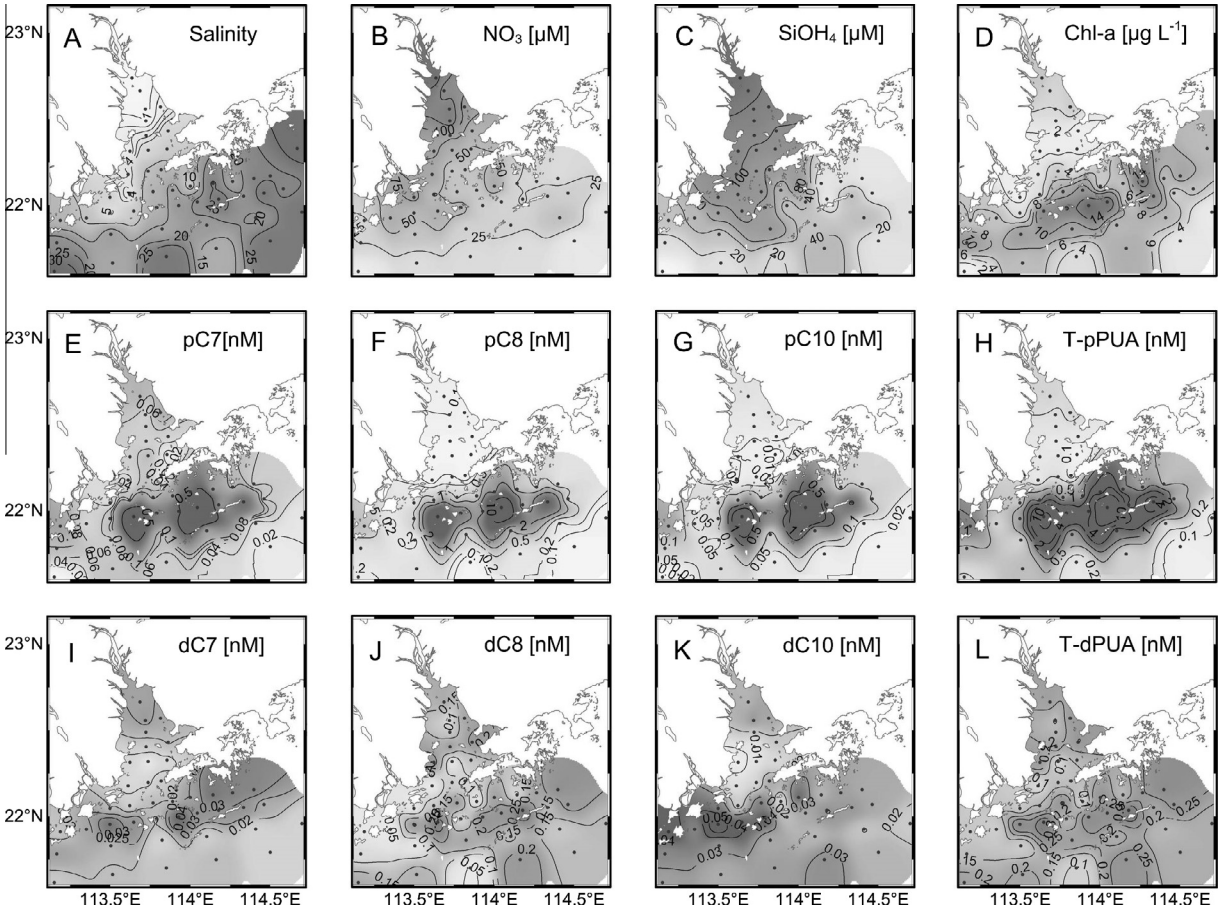

Fig. 2. Spatial distributions of (A) salinity, (B) NO_3, (C) $SiOH_4$, (D) chlorophyll-a (Chl-*a*), (E) particulate heptadienal (*p*C7), (F) particulate octadienal (*p*C8), (G) particulate decadienal (*p*C10), (H) total particulate PUA (T-*p*PUA), (I) dissolved heptadienal (*d*C7), (J) dissolved octadienal (*d*C8), (K) dissolved decadienal (*d*C10), and (L) total dissolved PUA (T-*d*PUA) in the Pearl River Estuary of the NSCS during June 2015.

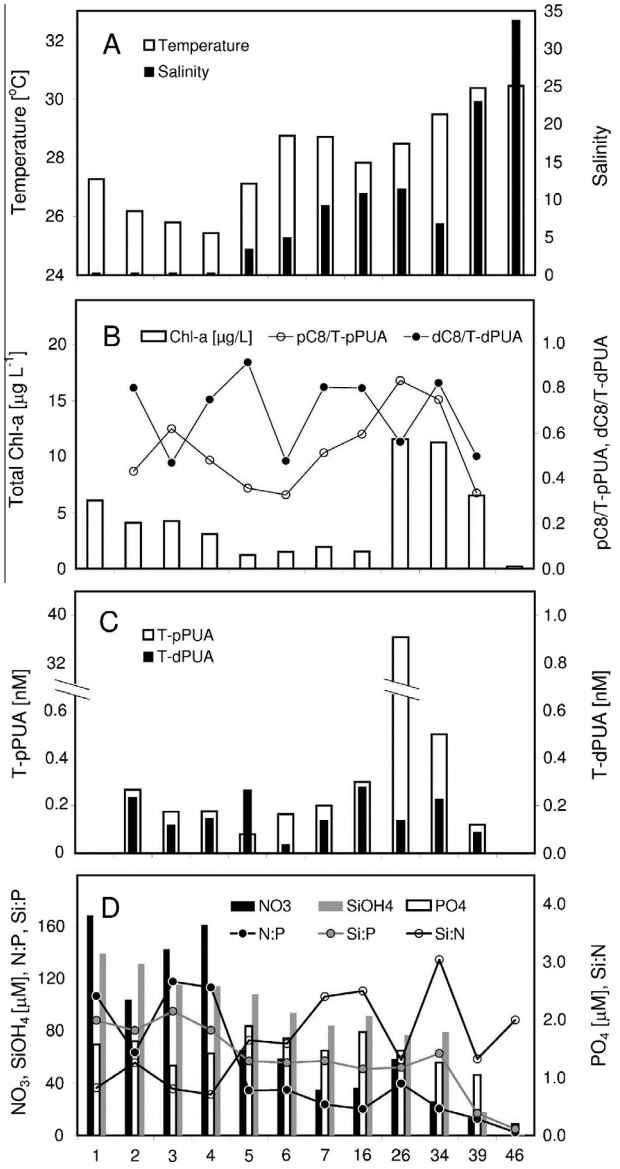

Fig. 3. Variations of (A) temperature and salinity, (B) total chlorophyll-*a* (Chl-*a*) and the ratios of *p*C8/T-*p*PUA and *d*C8/T-*d*PUA, (C) total particulate PUA (T-*p*PUA) and total dissolved PUA (T-*d*PUA), and (D) nutrients (NO_3, PO_4, $SiOH_4$) and nutrient ratios (N/P, Si/P, Si/N) for the along-PRE section from the Pearl River to the open NSCS during June 2015.

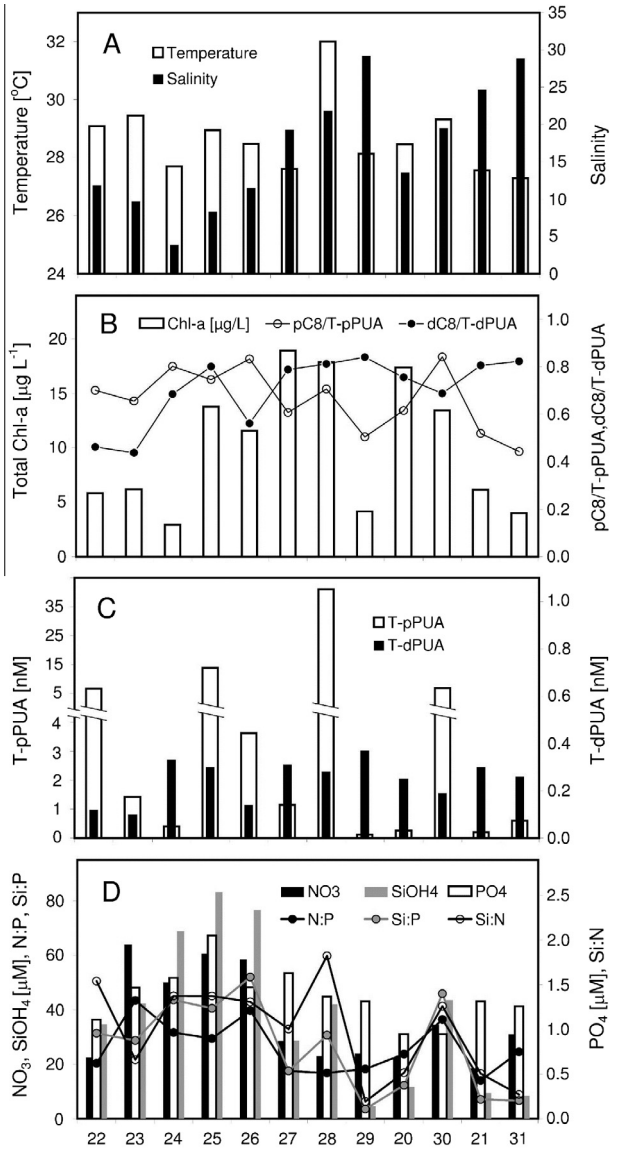

Fig. 4. Variations of (A) temperature and salinity, (B) total chlorophyll-*a* (Chl-*a*) and the ratios of *p*C8/T-*p*PUA and *d*C8/T-*d*PUA, (C) total particulate PUAs (T-*p*PUA) and total dissolved PUAs (T-*d*PUA), and (D) nutrients (NO_3, PO_4, $SiOH_4$) and nutrient ratios (N/P, Si/P, Si/N) for the across-PRE section in the NSCS in June 2015.

due to extremely high N/P ratios of the river inputs. There was an increased ratio of *p*C8 to T-*p*PUA within the chlorophyll bloom along the PRE (Fig. 3B), probably due to an elevated contribution of *S. costatum*. The low percentage of *p*C10 may reflect the relatively lower contributions of *p*C10-producing species, such as *Thalassiosira rotul* and *Chaetoceros compressus*, and *Phaeocystis* sp., to the summer phytoplankton blooms in the PRE (Wei et al., 2012; Zhang et al., 2013). Although there were large differences in concentrations of *p*C7, *p*C8, and *p*C10, their spatial distributions were quite similar in the PRE with two maximal concentrations on both the west and the east sides outside the estuary mouth (Fig. 2E–G). Concentrations of T-*p*PUA by the sum of *p*C7, *p*C8, and *p*C10 were highly variable, ranging from undetectable to >40 nM (Fig. 2H). Diatom PUA production is a dynamic process affected by a number of factors including hydrodynamics, nutrients, light, and cell cycles (Ribalet et al., 2007b).

There was a positive correlation between T-*p*PUA and chlorophyll-*a* with the six high-chlorophyll stations excluded ($r = 0.52$, $n = 37$, $p < 0.01$, Fig. 5A), suggesting the important role of phytoplankton for PUA production in the PRE. Following the change of surface chlorophyll-*a* (Fig. 3B), T-*p*PUA on the along-PRE section was very low in the estuary but high just outside the estuary mouth, before reaching sub-nanomolar levels offshore (Fig. 3C). Extremely high T-*p*PUA concentrations of 41, 13.87, 6.87 and 3.63 nM were found at stations 28, 25, 30 and 26, all located within the high-chlorophyll patches outside the PRE mouth (Fig. 4B and C). Previous cruises suggested that the high-chlorophyll zones of the PRE mouth were dominated by PUA-producing phytoplankton such as the diatom *S. costatum*, which produced T-*p*PUA by cell-lysis when experiencing serious physiological stresses, such as intense grazing. However, in contrast to these stations with increases of both T-*p*PUA and chlorophyll-*a*, stations 20 and 27 showed somewhat lower T-*p*PUA (0.26 and 1.14 nM), though chlorophyll-*a* there were among the highest (17.41 and 18.95 μg/L). Further investigation revealed that T-*p*PUA within the high chlorophyll patches (Fig. 4B and C) showed a good correlation with temperature (Fig. 5B), suggesting the crucial role

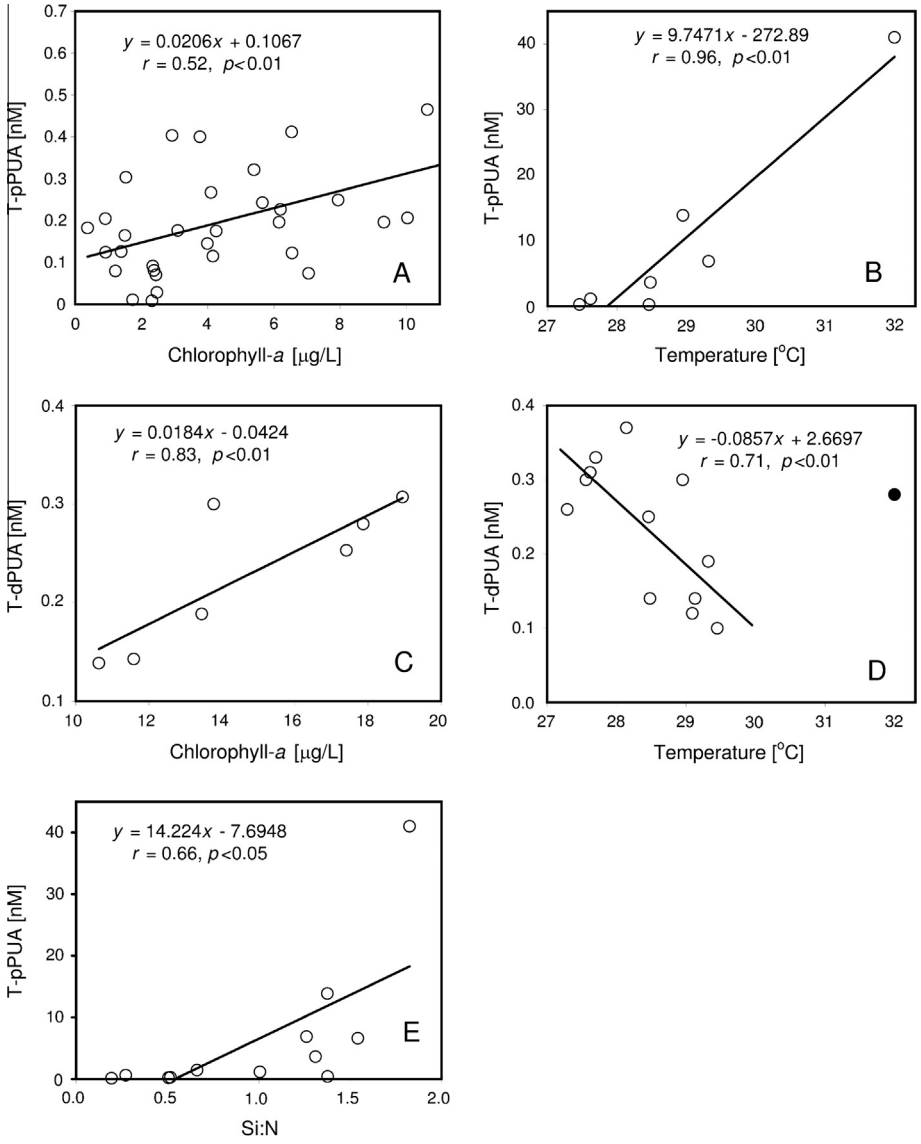

Fig. 5. Relationships of T-*p*PUA with (A) chlorophyll-*a* for non-blooming stations and with (B) temperature for blooming stations, together with the relationships of T-*d*PUA with (C) chlorophyll-*a* for blooming stations and with (D) temperature for the across-PRE section, as well as the relationships of T-*p*PUA with (E) Si/N ratio for the across-PRE section. Note that stations with chllorophyll-*a* >10 μgL^{-1} were defined as blooming stations with others defined as non-blooming stations.

of temperature on PUA production, likely through the temperature effect on diatom growth. Therefore, the high chlorophyll-*a* but low T-*p*PUA may reflect the constraint of lower temperature at stations 20 and 27. We however cannot rule out the presence of non PUA-producing species *N. pungens*, which is also an important diatom during the summer bloom (Huang et al., 2004).

Lipid compositions and enzyme activities could affect diatom PUA synthesis (Ribalet et al., 2007b), which would be less important in the eutrophic PRE. In fact, marine diatoms could have a wide range of PUA cell content depending on their nutrient status (Ribalet et al., 2009). There was a significant correlation between T-*p*PUA and the Si/N ratio ($r = 0.66$, $n = 12$, $p < 0.05$) for the across-PRE section (Fig. 5E), revealing the silicate control on diatom PUA production during the phytoplankton bloom. This result was different from previous finding of increasing particulate PUA production by diatom *S. marinoi* under strong silica stress in culture experiments (Ribalet et al., 2009), since there was less Si limitation in our across-PRE section as indicated by the relatively high Si/N and Si/P ratios. There are several other factors potentially affecting diatom PUA production in the PRE, including Fe and Ni limitations, UV radiation, and grazing. Micronutrients (Fe/Ni) are less likely to limit PUA production in the PRE, as they are generally replete in the estuary because of a heavy runoff. Diatom PUA production would likely be influenced by day-to-day change of UV radiation in the PRE in spite of the small area of the estuary. Zooplankton grazing could consume 27 ± 49% of primary productivity in the PRE (Tan et al., 2004). Therefore, the grazing impact may also affect the spatial distributions of diatoms and T-*p*PUA in the PRE.

3.3. Spatial distributions of dissolved PUAs in the surface waters

Total dissolved PUAs (T-*d*PUA) were less variable (0.10–0.37 nM), about two orders of magnitude lower than that of T-*p*PUA (0–41 nM), but were much higher than found in the North Atlantic Ocean (<1 pM; Bartual et al., 2014). Relatively higher T-*d*PUA was found in the bloom region outside the PRE (Fig. 2L), following the spatial distribution of T-*p*PUA (Fig. 2H). Dissolved octadienal (*d*C8) was ~73% of the T-*d*PUA in seawater with dissolved heptadienal (*d*C7) and decadienal (*d*C10) generally <13% and 15% (Fig. 2I–L), which agreed well with *p*PUAs (Fig. 2E–H). However,

unlike that of the *p*PUAs, the surface distributions of individual dissolved PUA (*d*C7, *d*C8, or *d*C10) differed substantially from one another (Fig. 2I–K). In contrast to the particulate PUAs produced during the exponential, stationary and declining phases of diatom growth, dissolved PUAs are released only during the late stationary period (Vidoudez and Pohnert, 2008). In agreement with *p*C7 (Fig. 2E), *d*C7 showed two maximal concentrations on both sides of the PRE (Fig. 2I), whereas the *d*C8 distribution was comparable to that of the surface chlorophyll-*a*, with elevated concentrations just outside the PRE (Fig. 2D). Interestingly, the highest concentration of *d*C10 was found in the southwest part of the PRE (Fig. 2K) where the freshwater outflow met the NSCS seawater (Fig. 2A).

The distributions of various chain-lengths of *d*PUAs in the PRE are consistent with the general summer phytoplankton community composition. Elevated concentrations of *d*C7 and *d*C8 at the PRE mouth can be explained by the perennial summer blooms of diatom *S. costatum* there (Huang et al., 2004; Harrison et al., 2008; Wei et al., 2012), which produces *d*C7 and *d*C8 but not *d*C10 (Vidoudez et al., 2011b). On the other hand, the spatial patterns of *d*PUAs may also reflect the variations of zooplankton grazing in the PRE. As a defensive reaction during sloppy grazing, *d*PUAs are released to seawater by damaged diatoms to repel further copepod grazing (Jüttner, 2005). Moreover, trace levels of *d*PUAs in seawater could be the result of PUA release upon lysis of dead diatom cells. Therefore, processes promoting cell-lysis of PUA-producing diatoms (Ribalet et al., 2014), such as nutrient limitation and the presence of viruses and algicidal bacteria, may also contribute to the spatial heterogeneity of *d*PUAs in the PRE.

There was a good correlation between T-*d*PUA and chlorophyll-*a* (Fig. 5C) for stations within the high-chlorophyll patches (Fig. 1), supporting the biological source of dissolved PUAs. Interestingly, we found higher T-*d*PUA at stations 24 and 29 (Fig. 4B and C), both located at the edge of the chlorophyll bloom. High T-*d*PUA but low chlorophyll in the north Adriatic Sea had been attributed to PUA-producing species other than diatoms or the high activity of PUA-producing enzymes after cell damage (Ribalet et al., 2014). Both enzymes and chlorophyll would be released to seawater from the wounded diatoms during copepod sloppy grazing (Pohnert, 2000). The major PUA-producing enzymes however could remain activated for a period of time in seawater (Pohnert, 2002) to continue production of dissolved PUAs. For the cross-PRE section (Fig. 4A and C), T-*d*PUA negatively correlated with temperature ($r = 0.71$, $p < 0.01$) when station 28 was not included because of its extremely high temperature (Fig. 5D). This result is in agreement with previous findings that the stability of dissolved PUAs would generally decrease with an increase of temperature (Bartual and Ortega, 2013). Although a temperature of 32 °C at station 28 was not favorable for the persistence of T-*d*PUA, the extremely high T-*p*PUAs resulted in a high concentration of T-*d*PUA in this station, thus falling away from the linear regression (Fig. 5C).

3.4. Ecological implications from the spatial variability of PUAs in the PRE and the adjacent NSCS

In the pelagic planktonic ecosystem with a short and efficient food chain, copepod grazing on diatoms is believed to be fundamentally important for transferring primary production to higher trophic levels (Calbet, 2001). What contradicts this classic view is the release of diatom toxins such as PUAs to impair copepod reproduction. Several factors will potentially affect the diatom-PUA-copepod relationship, including the self-defense of copepods to PUA toxicity (Lauritano et al., 2011), the species-specific variability of diatom PUA production (Wichard et al., 2005a), the temporal change of diatom clones (Taylor et al., 2009), and the shift of diatom physiology by nutrient limitation (Ribalet et al., 2009). Therefore, contradictory results have been reported with some showing clear deterrent effects of diatom PUAs on copepods, but others showing no correlations between PUA-producing diatoms and copepod reproduction (Ianora and Miralto, 2010).

At least three prerequisites exist for this diatom toxin effect to operate: high PUA concentrations, few prey alternatives, and copepods feeding on diatoms (Halsband-Lenk et al., 2005). All these prerequisites are well satisfied in our study area. In addition to the observed high levels of particulate and dissolved PUAs, the phytoplankton community of the eutrophic PRE was largely dominated by PUA-producing diatoms, particularly *S. costatum*, with copepods as the major grazer (Huang et al., 2004; Harrison et al., 2008; Liu et al., 2010). Through their impacts on diatom-copepod interaction, the high spatial variability of PUAs could be an important mechanism for shaping the plankton community structure of the PRE and the adjacent NSCS. Previous data crossing the diatom bloom outside the PRE mouth have shown unexpectedly low copepod abundances (Tan et al., 2004) associated with high chlorophyll-*a* and diatom biomass, although they were normally correlated at the edge of the bloom (see Fig. 6A). Our finding of high dissolved and particulate PUAs associated with the phytoplankton bloom in the PRE may explain the failure of copepods within the bloom region. Except for *N. pungens*, the other three major diatom species, including *S. costatum*, *N. delicatissima*, and *L. danicus* (Huang et al., 2004), are PUA-producing diatoms with much higher biomasses in the summer blooms (Fig. 6A).

Existing data revealed an inverse-relationship between PUA-producing diatom biomass and copepod abundance within the summer chlorophyll blooms at the PRE mouth during 1999, 2006, 2010, and 2011 (Fig. 6B). Although PUAs affect only the copepod larvae, their effects on copepod adults can be significant on a timescale longer than the reproductive period of copepod, generally about one week under favorable conditions (e.g. Caramujo and Boavida, 1999). These diatoms would be expected to have imposed high doses of PUAs on the indigenous copepods, leading to spatial variations of copepod abundances. It is likely that copepods here may move to feed on other phytoplankton such as dinoflagellates rather than on diatoms due to the PUAs produced during the bloom (Liu et al., 2010). Although the coupling between phytoplankton and mesozooplankton may decrease in the PRE due to environmental changes such as temperature, salinity, nutrient and light (Chen et al., 2011), our results suggest that PUA production by marine diatoms is an important driver for copepod distribution and grazing diversity in eutrophic coastal areas.

Using a relationship of particulate organic carbon (POC) and volume for diatom derived marine snow particles (Brzezinski et al., 1997), and a conservative Chl-*a*/POC ratio of 0.02 gChl gC^{-1} (He et al., 2010) in the PRE, we estimate the PUA concentrations in sinking particle to be 0–4 μM. Since our PUA estimations by freeze-thaw methods include the portion of PUAs within the particles eventually produced as cells die, the actual PUA concentrations outside the bacterial cells should be even lower. Still, this level of particulate PUAs could stimulate respiration and cell growth of particle-associated bacteria (Edwards et al., 2015). PUA-enhanced respiration of sinking POC would likely accelerate the transfer of organic carbon to inorganic carbon, leading to a decrease of POC export efficiency and thus affect the carbon cycle of the coastal oceans. On the other hand, the level of particulate PUAs in sinking particles might enhance the release rates of dissolved inorganic phosphorus (Edwards et al., 2015), contributing to the phytoplankton bloom outside the PRE by relieving phosphorus limitation of primary productivity, a common feature of the river plume due to high N/P ratios of the river outflows (Zhang et al., 1999; Yin et al., 2001).

The levels of PUAs reported in this study (0–41 nM T-*p*PUAs and 0.10–0.37 nM T-*d*PUAs) may be important for microbial

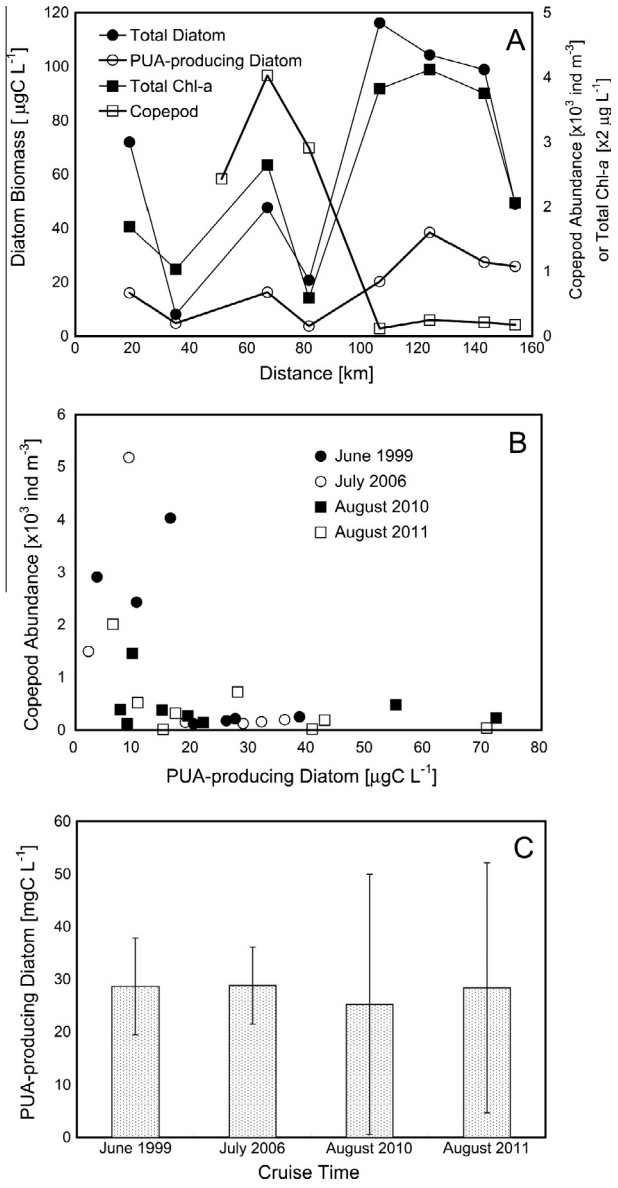

Fig. 6. (A) Variations of total diatom biomass, PUA-producing diatom biomass, total chlorophyll-*a*, and copepod abundance along a section at the PRE mouth in July 1999; (B) Relationship between copepod abundance and PUA-producing diatom biomass within the summer chlorophyll blooms at the PRE mouth during 1999, 2006, 2010 and 2011; (C) Average PUA-producing diatom biomass in chlorophyll blooms of different cruises. Location of the section for panel A is illustrated in Fig. 1. Diatom carbon biomasses are estimated by methods given in Section 2.5 with copepod abundances reproduced from literature data (see text for detail).

biogeochemistry of the PRE. It had been suggested that bacterioplankton groups would respond differently to the addition of 7.5 nM PUAs (Balestra et al., 2011). In particular, *Bacteroidetes* and *Rhodobacteraceae* were sensitive to the presence of low-level PUAs by decreasing their cell activities, while the growth and metabolic activities of *Gammaproteobacteria* and SAR11 were promoted by the PUA addition (Balestra et al., 2011). Both *Gammaproteobacteria* and SAR11 were relatively abundant in the bottom waters and in the anoxic sediments of the PRE (Sun et al., 2011; Liu et al., 2015). The PUA-enriched particles and surface seawater could be easily delivered to the bottom depths of 20–30 m near the PRE mouth by particle sinking and wind-induced vertical mixing (Yin et al., 2004a). Therefore, the stimulating effect of PUAs on the dominant bacterioplankton groups (*Gammaproteobacteria* and SAR11) would increase oxygen consumption by utilizing local organic carbon and thus exacerbate the low oxygen conditions in bottom waters outside the PRE mouth. There are often zones of reduced oxygen below the summer phytoplankton bloom outside the PRE mouth (Yin et al., 2004b), a transient phenomenon due to the interplay between biological processes, including organic carbon production and respiration, and physical processes, such as a reduced vertical mixing and a slower estuarine flushing rate (Harrison et al., 2008). These potential PUA impacts on eutrophic estuaries may result in a long-term alteration of the coastal ecosystem and biogeochemical cycles of the PRE and the adjacent NSCS.

4. Conclusions

We have reported the first comprehensive field survey of dissolved and particulate PUAs in the PRE and the adjacent NSCS along with complex physical and biogeochemical measurements. Our results reveal high levels of particulate (0–41 nM) and dissolved PUAs (0.10–0.37 nM) in the study region with substantial spatial variability. T-*p*PUA showed a strong correlationship with temperature within the intense phytoplankton bloom outside the PRE mouth, although it was generally positively correlated with chlorophyll-*a* over the entire region. We also found a significant correlation between T-*p*PUA and the Si/N ratio along the estuary, indicating silica control of diatom PUA production in the eutrophic estuary. T-*d*PUA showed a positive correlation with chlorophyll-*a* within blooms, but a negative correlation with temperature outside blooms, reflecting the complex physical and biological effects on the distribution of dissolved PUAs in the ocean. The high PUAs observed in the bloom region, together with an inverse-relationship between PUA-producing diatom and copepod there, suggests the essential role of PUAs in diatom-copepod interactions and grazing activity within the eutrophic estuary. High PUAs are also expected to affect the carbon cycle of coastal NSCS by decreasing POC export and increasing organic phosphorus remineralization. Finally, by stimulating bacterioplankton oxygen utilizations, the observed nanomolar levels of PUAs would strengthen the oxygen depletion of bottom waters outside the PRE mouth.

Acknowledgments

We thank two anonymous reviewers for their constructive comments. We are grateful to Prof. C. Zhang (SCSIO) and Prof. W.M. Zhang (GIM) for analytical assistances. This work was supported by the Chinese Recruitment Program of Global Experts and the National Key Research and Development Program of China (2016YFA0601203-02) to QPL and by an award of Natural Science Foundation of Guangdong Province to ZW (2014A030310353).

References

Balestra, C., Alonso-Saez, L., Gasol, J.M., Casotti, R., 2011. Group-specific effects on coastal bacterioplankton of polyunsaturated aldehydes produced by diatoms. Aquatic Microbial Ecology 63, 123–131.

Bartual, A., Arandia-Gorostidi, N., Cozar, A., Morillo-Garcia, S., Jesus Ortega, M., Vidal, M., Maria Cabello, A., Ignacio Gonzalez-Gordillo, J., Echevarria, F., 2014. Polyunsaturated aldehydes from large phytoplankton of the Atlantic Ocean surface (42 degrees N to 33 degrees S). Marine Drugs 12, 682–699.

Bartual, A., Ortega, M.J., 2013. Temperature differentially affects the persistence of polyunsaturated aldehydes in seawater. Environmental Chemistry 10, 403–408.

Brzezinski, M.A., Alldredge, A.L., O'Bryan, L.M., 1997. Silica cycling within marine snow. Limnology and Oceanography 42, 1706–1713.

Brzezinski, M.A., 2008. Mining the diatom genome for the mechanism of biosilicification. Proceedings of the National academy of Sciences of the United States of America 105, 1391–1392.

Cai, W.J., Dai, M.H., Wang, Y.C., Zhai, W.D., Huang, T., Chen, S.T., Zhang, F., Chen, Z.Z., Wang, Z.H., 2004. The biogeochemistry of inorganic carbon and nutrients in the Pearl River estuary and the adjacent northern South China Sea. Continental Shelf Research 24, 1301–1319.

Calbet, A., 2001. Mesozooplankton grazing effect on primary production: a global comparative analysis in marine ecosystems. Limnology and Oceanography 7, 1824–1830.
Caldwell, G.S., 2009. The influence of bioactive oxylipins from marine diatoms on invertebrate reproduction and development. Marine Drugs 7, 367–400.
Caramujo, M.J., Boavida, M.J., 1999. Characteristics of the reproductive cycles and development times of *Copidodiaptomus numidicus* (Copepoda: Calanoida) and *Acanthocyclops robustus* (Copepoda: Cyclopoida). Journal of Plankton Research 21, 1765–1778.
Chen, M., Chen, B., Harrison, P., Liu, H., 2011. Dynamics of mesozooplankton assemblages in subtropical coastal waters of Hong Kong: a comparative study between a eutrophic estuarine and a mesotrophic coastal site. Continental Shelf Research 31, 1075–1086.
Dutz, J., Koski, M., Jonasdottir, S.H., 2008. Copepod reproduction is unaffected by diatom aldehydes or lipid composition. Limnology and Oceanography 53, 225–235.
Edwards, B.R., Bidle, K.D., van Mooy, B.A.S., 2015. Dose-dependent regulation of microbial activity on sinking particles by polyunsaturated aldehydes: implications for the carbon cycle. Proceedings of the National academy of Sciences of the United States of America 112, 5909–5914.
Frost, B.W., 2005. Diatom blooms and copepod responses: paradigm or paradox? Progress in Oceanography 67, 283–285.
Halsband-Lenk, C., Pierson, J.J., Leising, A.W., 2005. Reproduction of *Pseudocalanus newmani* (Copepoda: Calanoida) is deleteriously affected by diatom blooms – a field study. Progress in Oceanography 67, 332–348.
Hansen, H.P., Koroleff, F., 1999. Determination of nutrients. In: Methods of Seawater Analysis, third ed. Wiley, Weinheim, pp. 159–228.
Harrison, P.J., Yin, K., Lee, J.H.W., Gan, J., Liu, H., 2008. Physical-biological coupling in the Pearl River Estuary. Continental Shelf Research 28, 1405–1415.
Harrison, P.J., Zingone, A., Mickelson, M.J., Lehtinen, S., Ramaiah, N., Kraberg, A.C., Sun, J., McQuatters-Gollop, A., Jakobsen, H.H., 2015. Cell volumes of marine phytoplankton from globally distributed coastal data sets. Estuarine, Coastal and Shelf Science 162, 130–142.
He, B., Dai, M., Zhai, W., Wang, L., Wang, K., Chen, J., Lin, J., Han, A., Xu, Y., 2010. Distribution, degradation and dynamics of dissolved organic carbon and its major compound classes in the Pearl River estuary, China. Marine Chemistry 119, 52–64.
Huang, L.M., Jian, W.J., Song, X.Y., Huang, X.P., Liu, S., Qian, P.Y., Yin, K.D., Wu, M., 2004. Species diversity and distribution for phytoplankton of the Pearl River estuary during rainy and dry seasons. Marine Pollution Bulletin 49, 588–596.
Ianora, A., Miralto, A., 2010. Toxigenic effects of diatoms on grazers, phytoplankton and other microbes: a review. Ecotoxicology 19, 493–511.
Jüttner, F., 2005. Evidence that polyunsaturated aldehydes of diatoms are repellents for pelagic crustacean grazers. Aquatic Ecology 39, 271–282.
Lauritano, C., Borra, M., Carotenuto, Y., Biffali, E., Miralto, A., Procaccini, G., Ianora, A., 2011. Molecular evidence of the toxic effects of diatom diets on gene expression patterns in copepods. PLoS ONE 6. http://dx.doi.org/10.1371/journal.pone.0026850.
Li, G., Lin, Q., Lin, J., Song, X., Tan, Y., Huang, L., 2014. Environmental gradients regulate the spatial variations of phytoplankton biomass and community structure in surface water of the Pearl River estuary. Acta Ecologica Sinica 34, 129–133.
Lian, X., Tan, Y., Liu, Y., Huang, L., Chen, Q., Zhou, L., 2013. Comparison of capture efficiency for zooplankton in the northern South China Sea, using two plankton mesh sizes (in Chinese). Journal of Tropical Oceanography 32, 33–39.
Liu, H., Chen, M., Suzuki, K., Wong, C.K., Chen, B., 2010. Mesozooplankton selective feeding in subtropical coastal waters as revealed by HPLC pigment analysis. Marine Ecology Progress Series 407, 111–123.
Liu, J., Fu, B., Yang, H., Zhao, M., He, B., Zhang, X.-H., 2015. Phylogenetic shifts of bacterioplankton community composition along the Pearl Estuary: the potential impact of hypoxia and nutrients. Frontiers in Microbiology 6. http://dx.doi.org/10.3389/fmicb.2015.00064.
Mao, Q.W., Shi, P., Yin, K.D., Gan, J.P., Qi, Y.Q., 2004. Tides and tidal currents in the pearl river estuary. Continental Shelf Research 24, 1797–1808.
Miralto, A., Barone, G., Romano, G., Poulet, S.A., Ianora, A., Russo, G.L., Buttino, I., Mazzarella, G., Laabir, M., Cabrini, M., Giacobbe, M.G., 1999. The insidious effect of diatoms on copepod reproduction. Nature 402, 173–176.
Morillo-Garcia, S., Valcarcel-Perez, N., Cozar, A., Ortega, M.J., Macias, D., Ramirez-Romero, E., Garcia, C.M., Echevarria, F., Bartual, A., 2014. Potential polyunsaturated aldehydes in the strait of Gibraltar under two tidal regimes. Marine Drugs 12, 1438–1459.
Pan, J.Y., Gu, Y.Z., Wang, D.X., 2014. Observations and numerical modeling of the Pearl River plume in summer season. Journal of Geophysical Research-Oceans 119, 2480–2500.
Parsons, T.R., Maita, Y., Lalli, C.M. (Eds.), 1984. A manual of Chemical and Biological Methods for Seawater Analysis. Pergamum Press, Oxford.
Pohnert, G., 2000. Wound-activated chemical defense in unicellular planktonic algae. Angewandte Chemie-International Edition 39, 4352–4354.
Pohnert, G., 2002. Phospholipase A(2) activity triggers the wound-activated chemical defense in the diatom *Thalassiosira rotula*. Plant Physiology 129, 103–111.
Ribalet, F., Bastianini, M., Vidoudez, C., Acri, F., Berges, J., Ianora, A., Miralto, A., Pohnert, G., Romano, G., Wichard, T., Casotti, R., 2014. Phytoplankton cell lysis associated with polyunsaturated aldehyde release in the northern Adriatic Sea. PLoS ONE 9, e85947. http://dx.doi.org/10.1371/journal.pone.0085947.
Ribalet, F., Berges, J.A., Ianora, A., Casotti, R., 2007a. Growth inhibition of cultured marine. Phytoplankton by toxic algal-derived polyunsaturated aldehydes. Aquatic Toxicology 85, 219–227.
Ribalet, F., Wichard, T., Pohnert, G., Ianora, A., Miralto, A., Casotti, R., 2007b. Age and nutrient limitation enhance polyunsaturated aldehyde production in marine diatoms. Phytochemistry 68, 2059–2067.
Ribalet, F., Vidoudez, C., Cassin, D., Pohnert, G., Ianora, A., Miralto, A., Casotti, R., 2009. High plasticity in the production of diatom-derived polyunsaturated aldehydes under nutrient limitation: physiological and ecological implications. Protist 160, 444–451.
Sarno, D., Kooistra, W., Medlin, L.K., Percopo, I., Zingone, A., 2005. Diversity in the genus *Skeletonema* (Bacillariophyceae). II. An assessment of the taxonomy of *S. costatum*-like species with the description of four new species. Journal of Phycology 41, 151–176.
Sun, F.-L., Wang, Y.-S., Wu, M.-L., Wang, Y.-T., Li, Q.P., 2011. Spatial heterogeneity of bacterial community structure in the sediments of the Pearl River estuary. Biologia 66, 574–584.
Tan, Y.H., Huang, L.M., Chen, Q.C., Huang, X.P., 2004. Seasonal variation in zooplankton composition and grazing impact on phytoplankton standing stock in the Pearl River Estuary, China. Continental Shelf Research 24, 1949–1968.
Taylor, R.L., Abrahamsson, K., Godhe, A., Wangberg, S.A., 2009. Seasonal variability in polyunsaturated aldehyde production potential among strains of *Skeletonema marinoi* (Bacillariphyceae). Journal of Phycology 45, 46–53.
Tosti, E., Romano, G., Buttino, I., Cuomo, A., Ianora, A., Miralto, A., 2003. Bioactive aldehydes from diatoms block the fertilization current in ascidian oocytes. Molecular Reproduction and Development 66, 72–80.
Vidoudez, C., Casotti, R., Bastianini, M., Pohnert, G., 2011a. Quantification of dissolved and particulate polyunsaturated aldehydes in the Adriatic Sea. Marine Drugs 9, 500–513.
Vidoudez, C., Nejstgaard, J.C., Jakobsen, H.H., Pohnert, G., 2011b. Dynamics of dissolved and particulate polyunsaturated aldehydes in mesocosms inoculated with different densities of the diatom *Skeletonema marinoi*. Marine Drugs 9, 345–358.
Vidoudez, C., Pohnert, G., 2008. Growth phase-specific release of polyunsaturated aldehydes by the diatom *Skeletonema marinoi*. Journal of Plankton Research 30, 1305–1313.
Wei, G., Wang, H., Cai, W., Yi, B., 2012. 10-year retrospective analysis on the harmful algal blooms in the Pearl River Estuary (in Chinese). Marine Science Bulletin 31, 466–474.
Wichard, T., Poulet, S.A., Halsband-Lenk, C., Albaina, A., Harris, R., Liu, D., Pohnert, G., 2005a. Survey of the chemical defence potential of diatoms: screening of fifty species for α, β, γ, δ-unsaturated aldehydes. Journal of Chemical Ecology 31, 949–958.
Wichard, T., Poulet, S.A., Pohnert, G., 2005b. Determination and quantification of alpha, beta, gamma, delta-unsaturated aldehydes as pentafluorobenzyl-oxime derivates in diatom cultures and natural phytoplankton populations: application in marine field studies. Journal of Chromatography B-Analytical Technologies in the Biomedical and Life Sciences 814, 155–161.
Wichard, T., Poulet, S.A., Boulesteix, A.-L., Ledoux, J.B., Lebreton, B., Marchetti, J., Pohnert, G., 2008. Influence of diatoms on copepod reproduction. II. Uncorrelated effects of diatom-derived alpha, beta, gamma, delta-unsaturated aldehydes and polyunsaturated fatty acids on *Calanus helgolandicus* in the field. Progress in Oceanography 77, 30–44.
Yin, K.D., Qian, P.Y., Wu, M.C.S., Chen, J.C., Huang, L.M., Song, X.Y., Jian, W.J., 2001. Shift from P to N limitation of phytoplankton growth across the Pearl River estuarine plume during summer. Marine Ecology Progress Series 221, 17–28.
Yin, K.D., Zhang, J.L., Qian, P.Y., Jian, W.J., Huang, L.M., Chen, J.F., Wu, M.C.S., 2004a. Effect of wind events on phytoplankton blooms in the Pearl River estuary during summer. Continental Shelf Research 24, 1909–1923.
Yin, K.D., Lin, Z.F., Ke, Z.Y., 2004b. Temporal and spatial distribution of dissolved oxygen in the Pearl River Estuary and adjacent coastal waters. Continental Shelf Research 24, 1935–1948.
Zhang, J., Yu, Z.G., Wang, J.T., Ren, J.L., Chen, H.T., Xiong, H., Dong, L.X., Xu, W.Y., 1999. The subtropical Zhujiang (Pearl River) Estuary: nutrient, trace species and their relationship to photosynthesis. Estuarine, Coastal and Shelf Science 49, 385–400.
Zhang, X., Shi, Z., Huang, X., Ye, F., Liu, Q., 2013. Phytoplankton abundance and size-fractionated structure in three contrasting periods in the Pear River Estuary. Journal of Marine Research 71, 187–210.
Zhang, X., Zhang, J., Huang, X., Huang, L., 2014. Phytoplankton assemblage structure shaped by key environmental variables in the Pearl River Estuary, South China. Journal of Ocean University of China 13, 73–82.
Zu, T., Wang, D., Gan, J., Guan, W., 2014. On the role of wind and tide in generating variability of Pearl River plume during summer in a coupled wide estuary and shelf system. Journal of Marine Systems 136, 65–79.